Perturbations to astronomical observations at the European Southern Observatory's very large telescope site in Paranal, Chile: analyses of climatological causes

Martin Beniston[1], Paula Casals[1], and Marc Sarazin[2]

1: Department of Geosciences, University of Fribourg, Switzerland

2: European Southern Observatory, Garching, Germany

Abstract

A study has been conducted to assess the reasons for a significant decrease in the astronomic observing period since the Very Large Telescope of ESO (the European Southern Observatory) went into operation in 1998. Following a multi-year monitoring of meteorological parameters at the site of the ESO telescope in Paranal (northern Chile), the optimal climatic conditions observed there prior to the construction of the Very Large Telescope have not been as frequently recorded since.

In order to determine whether this region is being subjected to long-term changes in climate consecutive to 20th century global warming, or whether the ENSO (El Niño/Southern Oscillation) event in the final years of the 1990s are responsible for this situation, climatological data from *in situ* measurements, upper-air soundings, analogical reconstructions of meteorological data to extend the records further back into the past, and large-scale re-analysis data have been used. The results point towards a dominant role of ENSO in the current problems that astronomers face with reduced observation time.

1. Introduction

Prior to setting up its Very Large Telescope (VLT) in Chile, the European Southern Observatory (ESO) undertook a multi-year climatological assessment of the Paranal site in terms of its suitability for astronomical observations (cloudiness, atmospheric turbidity, thermal turbulence, etc.). The site was deemed exceptional in terms of the quality and duration of conditions related to ground-based astronomical observations.

Following the construction and start of operations of ESO's VLT in 1998, however, atmospheric conditions have been considerably different from those recorded during the measurement period earlier in the 1990s (ESO, 2001). These shifts in climatic patterns, which have over the last few years significantly reduced observational capability compared to that expected from the multi-year climatological assessment, pose the following questions:

- Are these new climatic conditions totally anomalous and related to global warming?

- Are they dominated by ENSO events?
- Are they part of a cycle that has already occurred in the past but which was not recorded during the 15-year observation period at Paranal?

This paper attempts to answer these questions based on data analysis. Because the time-series at the ESO site are too short for any meaningful climatological statistics to be compiled, a first step in this investigation was to obtain additional observational data from other sites in order to check the consistency between longer-term records and the short 15-year ESO data set. Extending the data record helps provide key answers as to whether the current weather patterns are anomalous or not, against the backdrop of longer-term climate data.

Analysis from the NCAR-NCEP (National Center for Atmospheric Research/National Centers for Environmental Prediction) data also provides a synoptic overview to explain shifts in climatic conditions at Paranal. Such shifts include the circulation patterns that can favor or perturb the duration of astronomical observing periods.

This paper will thus report on the investigations based on the available climatological information; following an overview of the data and the methodologies used, the possible causal mechanisms leading to perturbations in astronomical observing periods will be discussed in more detail.

2. Climate and data

Much of the climate of South America is influenced by robust surface pressure patterns and the migration of the inter-tropical convergence zone, which affects large areas of tropical South America. The southern part of the continent is affected by anticyclonic conditions that prevail over both the Atlantic and the Pacific, the thermally-induced low pressure system of northwestern Argentina, and the mid-latitudes westerlies. All of these circulation features interact strongly with the Andean mountain chain. The behavior of the Southern Oscillation is responsible for much of the climate variability observed at interannual scales on the continent. Changes in circulation patterns observed during the 20th century are often associated with El Niño and La Niña events. Indeed, over much of South America, atmospheric circulation patterns are generally more perturbed during El Niño than during La Niña years (Salles and Compagnucci, 1997).

Precipitation in northern Chile normally occurs during the winter months. However, during early stages of the warm phase of ENSO, precipitation tends to be above-average; nevertheless, the region remains essentially semi-arid to extremely arid (Compagnucci, 1991; Ruttland and

Fuenzalida, 1991). When El Niño conditions prevail, strong rainfall events tend to occur at low elevations along the coastal ranges of Chile. Because the arid zone is not adapted to heavy precipitation, these events are capable of triggering debris flows such as those that affected Santiago and much of the coastal zone during the El Niño events of 1991-1993 (Garreaud and Ruttland, 1996) and 1997. North of 40°S in Chile, streamflows are above normal during El Niño years (Waylen and Caviedes, 1990; Compagnucci and Vargas, 1998; Compagnucci, 2000), as a result of higher rainfall and, at the highest elevations in the Andes, snowfall amounts; the reverse is true during La Niña years. Compagnucci and Vargas (1998) note that the likelihood of dry conditions during La Niña in northern Chile is generally higher than the likelihood of wet conditions during El Niño, however.

Cerro Paranal is located at 24°40'S and 70°25'W at an altitude of 2,635 m above sea-level (Figure 1). It is located in a region that is characterized by a dry coastal zone bordering a cold ocean current, and a coastal escarpment that rises to about 1,500 m. The escarpment acts as a barrier to the inland incursion of the moist marine boundary layer, where persistent stratus and strato-cumulus clouds are adominant feature. Above the escarpment lie the crests of the coastal ranges, which are located to the west of the Andean chain proper. In this arid piedmont zone, moderate temperatures prevail throughout the year; precipitation increases in summer and with height, from a few mm at around 3,000 m height to over 400 mm/year on the high Altiplano (Ruttland and Ulriksen, 1979). Convective activity is enhanced at certain periods of the year as a result of a feature known as the "Bolivian Winter", whereby a continental low-pressure pattern develops at latitudes located between 10°-30°S and centered on the 65°W meridian (van Loon et al., 1972). Upper-level tropical easterlies associated with the Bolivian low can occasionally lead to an advection of moisture that extends as far as the crests of the coastal ranges, down to altitudes of 2,500 m above sea level (Ruttland and Ulriksen, 1979).

Insert Figure 1 here

The time-series of available data at Paranal span the period from 1985 until present with, however, a number of gaps in the series that reflect occasional technical problems. In order to close these gaps, longer-term records have been used as will be discussed later, namely those from Antofagasta, located on the Pacific coast relatively close to Paranal.

The astronomy community uses a number of parameters to define the quality of atmospheric conditions favorable for astronomical observations. One such parameter that provides a measure of the quality of ground-based astronomical observations is termed *seeing*, which is the parameter that astronomers employ to describe the sky's atmospheric conditions. Seeing is the

effect of random variations of the index of refraction in the atmosphere on the quality of the image of an astronomic object; it is measured in arc-seconds. Because the atmosphere is in continual motion with changing temperatures, air currents and turbulence, weather fronts and dust particles combine to cause star images to shimmer (twinkle). If the stars are twinkling considerably, seeing conditions are poor, and the reverse is true when the star images are steady. The effects of poor seeing upon visual observation are, principally, small and erratic movements of the object and diffusion of its image. Atmospheric temperature and vertical stratification, in addition to turbulence, are thus the key elements that can influence seeing.

Insert Figure 2 here

At the Paranal site, there are several sets of missing data in the time series of the seeing parameter, as seen in Figure 2. However, several distinct periods can be identified, namely 1987-1991, 1993-1995, 1996-1997, and 1998-2001. A switch to much higher values of seeing occur after the beginning of 1998. As this is not a bias imposed by instrumental or site changes, it can be speculated that this shift in seeing has been triggered by a significant change in climatic regimes, as will be discussed later. Figure 2 also shows that, irrespective of variability on multi-year time-scales, there is also an annual cycle that is linked to differences in summer and winter regimes. These influence wind velocity and associated turbulence, as well as moisture and temperature characteristics at locations such as Paranal (see for example Garreaud and Battisti, 1999).

Insert Figure 3 here

The mean seeing for the period between April 1987 and August 1998 is 0.7. Figure 3 highlights the periods during which seeing is either above or below this mean value. In general, prior to 1996, conditions were considered excellent with occasional seasonal exceptions. However, since 1996, the seeing parameter has been systematically measured above 0.7. It has even exceeded 1.0 for several months since 1998; the highest value of the series was recorded in October 1998 (1.053). Even episodic improvements in 1999 and 2000 (0.759 in April 1999 and 0.808 in March 2000, for example) have been short-lived; the seeing parameter has not reverted to the low values characteristic of the pre-1996 period. Higher values of seeing are associated with a reduction in the quality of astronomical observations. Indeed, ESO considers that visibility deteriorated significantly from August 1998; a marginal amelioration was recorded in the latter part of the year 2000, with 0.712 in November 2000. Conditions have again deteriorated since then, however, with values exceeding 0.85 just 3 months later (February 2001).

Because the meteorological observations at Paranal span a relatively short time frame (1985-present), and because there are a number of gaps even in this short record, it is necessary to find an alternate method to close these gaps and to extend the Paranal record back in time. The main reason for undertaking this procedure is to allow an assessment of whether other periods in the past exhibit similar characteristics to those which have been causing problems for astronomical observations for the ESO VLT since the late 1990s.

Insert Figure 4 here

Analysis of the Paranal and Antofagasta records show that there is a synchronous behavior of the two time series, as seen in Figure 4; the correlation between the two sets of data is 0.77. This implies that climatic conditions at Paranal are also highly sensitive to ENSO conditions in the Pacific, despite the high elevation of the Paranal site and the fact that it is located well above the maritime boundary layer within which Antofagasta is embedded. It is thus legitimate and scientifically sound to use the Antofagasta temperature record as an analogy to reconstruct climate series at Paranal, taking into account the strong inversion that exists between sea-level and Paranal. Figure 5 provides an example for winter (May) given by the upper-air sounding at Antofagasta; it is seen that the inversion layer is systematically located between 800-1,200 m above sea-level and has a typical strength of 8°C. The two curves are provided for the best seeing conditions of the 1987-2001 period (May 1994) and worst seeing (May 1998). There is a difference of over 2°C between May 1998 and May 1994, which represents a systematic shift to cooler conditions at the time when seeing conditions are mediocre.

Insert Figure 5 here

Because temperature, thermal stratification, and its perturbation by turbulence are major determinants of seeing, an extension of the temperature record on the basis of the close correlation between Antofagasta and Paranal temperature data can help to identify possible periodicity and frequency of atmospheric disruptions of the quality of astronomical observations. Other meteorological variables, such as cloudiness or water vapor content will also affect night-time sky observations, but they play a lesser role in determining seeing, which is the parameter that ESO has identified as exhibiting the most significant deterioration in recent years.

Insert Figure 6 here

The long-term trend in temperature at Antofagasta is very low, at +0.11°C per century, based on the 1951-2000 time series given in Figure 6; in statistical terms, the trend is not significant. The

rate of warming at Antofagasta is almost one order of magnitude lower than the global-average warming observed since 1900 (Jones et al., 1999). At Paranal itself, over the short period of observational record, the warming trend is even less significant (+0.02°C per century, based on the 15 years of data). Direct regional warming linked to global climatic change can, at least on the basis of the available evidence, be ruled out as a significant driving factor for changes in astronomical observation conditions for the short period of record at Paranal.

Vuille and Bradley (2000) have investigated climatic trends from a number of sites in the Andes, from southern Chile northwards into Venezuela. They conclude that in the Tropical Andes, there are significant changes at high elevations that are for example leading to glacier retreat at an unprecedented rate. They also note that from 1933 to 1992, temperatures along the Chilean coast, averaged for stations located between 18°S and 35°S have increase up to 2°C per century, with an accelerating trend in the latter part of the record (Rosenblüth et al., 1997). This is apparently in contradiction with the present findings; most of the increase is seen to be in the minimum temperatures, however, which may not necessarily be reflected in the data sets used here for the Paranal and Antofagasta sites. Aceituno et al. (1993) report that surface air temperature has not shown consistent trends overall in Chile during the 20th century. They note that here has been a stepwise warming south of 45°S, but a cooling of up to 2°C from the 1950s to the mid-1970s from 35-45°S. Antofagasta and its neighboring mountain regions could thus be a particular exception to general warming or cooling trends. The Antofagasta region is perhaps a “pivotal” zone located between regions that have cooled just to the south (Aceituno et al., 1993), and that have warmed to the north (Vuille and Bradley, 2000).

The disproportionate rise of minimum temperatures compared to maximum temperatures during the 20th century is a feature that has been reported widely, both on global scales (e.g., Karl et al., 1993) and on local scales (e.g., Jungo and Beniston, 2001). Furthermore, long-term trends in climate have been shown by several authors (Giorgi et al., 1997; Vuille and Bradley, 2000) to have an altitudinal dependency that is not necessarily applicable to the Antofagasta and Paranal records. Caution therefore needs to be exercised in the interpretation of the sparse data available for this remote part of Chile. What is clear from past observations, however, is that important changes in zonal circulation have been observed over the last century, with weaker wintertime circulation for the period 1939-1949 and stronger circulations during 1967-1977. These changing patterns suggest interdecadal forcings (Hoffman *et al.*, 1987; Minetti and Sierra, 1989; Cantañeda and Barros, 1993; Barros *et al*., 1999) that are most certainly related to the behavior of the Southern Oscillation.

By looking at the two series in Figure 6, it can be surmised that other periods of lower than average seeing conditions have occurred in the past; those that are not included in the Paranal record may be captured by analogy with the Antofagasta record. An obvious example is the 1982-1983 El Niño event and the subsequent cold phase of ENSO, whose “signature” in this figure closely resembles that of the latest event in 1997 and subsequent years.

3. Results and discussion

The previous section has shown that long-term climatic change cannot be considered as the prime candidate to explain changes in seeing that have been responsible for less than optimal astronomical observing conditions since 1998. It would seem rather that the El Niño/Southern Oscillation (ENSO) mechanisms, which represent the dominant mode of climate variability in the region, may be responsible for the current situation. Furthermore, the poorer seeing conditions are clearly associated with the cold phase of ENSO and not the warm, El Niño phase. In the last ENSO event, the cold phase developed in mid-1998 and resulted in one of the strongest and most persistent La Niña events on record (Wolter and Timlin, 1998; McPhaden, 1999; Moore and Kleeman, 1999).

According to Garreaud and Battisti (1999), a teleconnection pattern associated with ENSO is located from the central tropical Pacific into the far southeastern Pacific Ocean; changes in this pattern influence the anomalies in the general circulation in the Southern Hemisphere. Such anomalies are generated by surface heat flux changes at the ocean-atmosphere interface, and thus can considerably modify the atmospheric conditions in northern Chile. Diaz and Graham (1996) have also shown that fluctuations in tropical freezing height levels are closely linked to the behavior of Pacific sea-surface temperatures; the influence of ENSO is transmitted to high-elevation sites in the Andes with a lag of 1-2 months, generally, as identified by Vuille et al. (2000). The 1997 event and the subsequent La Niña phase have been discussed in the scientific literature in terms of the possible links between changing ENSO periodicity and global warming (Eltahir and Wang, 1999; Hunt, 1999).

The large-scale patterns of convective cloudiness and circulation associated with interannual variability of summer rainfall over this region are related to the seasonal mean large-scale zonal flow over the central Andes. When easterly flow prevails over the region, it tends to favor the occurrence of summertime deep convection on the Altiplano through moist air advection from the interior of the continent, as indicated by Garreaud and Aceituno (2001). The authors furthermore suggest that interannual variability of the seasonal-mean zonal wind accounts for roughly 50% of

the variance of summertime convection over the Altiplano, with alternating moist easterly and dry westerly flows. The relationship between ENSO and interannual rainfall variability over the Altiplano can be explained by the warming of the tropical troposphere during the negative phase of ENSO and the associated strengthening of the westerlies over the central Andes. The reverse tends to occur during the warm, El Niño phase of ENSO (Garreaud and Aceituno, 2001).

In order to highlight the role of the warm and cold phases of ENSO at the Paranal site itself, two particular periods have been selected, namely those with the best and the worst conditions for astronomical observations. Based on the Paranal records for spring (October) and autumn (May), it is seen that the worst seeing conditions of the record are observed in October 1998 and in May 2000 while conversely, the most optimal seeing conditions occur in May 1994 and October 1994. The discussion will thus focus on the differences in the monthly means of large-scale and regional scale atmospheric patterns between these extremes to determine whether there is a systematic bias in synoptic weather conditions between periods when La Niña conditions prevail, and other climatic situations. Four climate-relevant variables are considered in this section, namely:

- geopotential height
- wind velocity and direction
- relative humidity
- cloud-induced net long-wave radiation. This latter parameter allows an indirect measure of the presence of clouds as a result of the reduction of outgoing terrestrial radiation that clouds exert.

3.1 Geopotential height analyses

A typical La Niña is accompanied by a tongue of colder-than-average SSTs in the tropical southern Pacific. A zone of relatively high pressure builds up to the south of the cold tongue, exemplified by a thickening of the layer and an upward shift of the 700 hPa pressure surface (Garreaud and Battisti, 1999). The 700 hPa geopotential height is the standard pressure level closest to the altitude of Paranal (2,635 m above sea level). This middle atmosphere pressure system is located south of about 20-25° S, off the western coast of Chile (see Figure 7a for May 2000 and 7b for October 1998). The height of the 700 hPa level is on average 3,140 m, and thus the height anomaly at the center of the high-pressure system is about 40 m, which represents a strong departure from mean geopotential height.

Insert Figure 7 here

Over Bolivia and southern Brazil, a secondary cell of high pressure is also observed, more extended in October 1998 than in May 2000, which may be related to the particular intensity of La Niña recorded in October 1998. A trough of lower geopotential values is located between the two

large-scale pressure patterns, whose negative anomalies can exceed 10 hPa. This middle-troposphere trough is oriented SE-NW, stretching from the Santiago area well into the tropical Pacific, far offshore from Ecuador and Peru. At Paranal itself, the geopotential height anomalies during the two selected La Niña months reach –6 to –10 m. The general flow pattern at the 700 hPa level, unperturbed by orography, is parallel to the isopotential lines, with lower heights located to the right of the flow direction.

Hence, synoptic flow enters the Paranal area from a WNW-NW direction, bringing with it characteristics of air originating close to the Equatorial zone above the Pacific. The close-up maps of the geopotential for the central part of South America, given in Figures 8a for May 2000 and 8b for October 1998, emphasize this general tendency. Further south, the flow is essentially of a westerly nature, typical of the middle latitude circulations.

Insert Figure 8 here

During the optimal seeing conditions of May and October, 1994, the synoptic situation is considerably different from that just described, as shown in Figures 9a and 9b, respectively. The high-pressure system over the eastern Pacific is either non-existent or much weaker and located further west over the Pacific than during El Niño, whereas the high-pressure system over Brazil is shifted further to the east. In May 1994 (Figure 9a), for example, this high-pressure cell is even located offshore of Brazil in the southern Atlantic. The direction of the synoptic flows is essentially from the W, with a slightly more WNW component in the case of May 1994. However, the source region from which these middle-tropospheric winds blow is located far to the south of the source region during the La Niña phase, so that the atmospheric characteristics advected along the 700 hPa surfaces are significantly different from those occurring during La Niña. Figures 10a and 10b for May 1994 and October 1994, respectively, show the close-up details of the 700 hPa geopotential height for central South America. In October 1994, a slight upper-air ridge located to the NW essentially decouples air flows reaching Paranal from the tropical Pacific, which is the exact opposite to what is observed during the La Niña phase.

Insert Figure 9 here

Insert Figure 10 here

3.2 Wind speed analyses

Because turbulence is essentially proportional to the square of wind speed, an increase in mechanical turbulence resulting from higher wind velocities may be expected, thereby generating

disturbances in atmospheric stratification, thus resulting in more shimmering. In addition, the NW orientation of the flow under La Niña conditions allows the air to be in contact over a longer distance (i.e., for a longer time) with the roughness elements of the continental surface than when the flow is oriented in a westerly direction. In the case of westerly flows, air transits from the ocean to the Paranal area with a minimum fetch over land, with a corresponding lowering of the potential for roughness-induced turbulence.

Insert Figure 11 here

It is seen from Figure 11 that, during La Niña conditions (represented in this study by October 1998 and May 2000), wind velocities are substantially higher at the altitude of the Paranal observatory. During “normal” conditions, associated with good seeing conditions (e.g., 1994), wind velocities are 4 m/s or less in the free atmosphere, while during the recent La Niña phase, wind velocities exceed 6 m/s. The energy potential for generating atmospheric turbulence thus increases by a factor of 2.5 between normal and La Niña conditions. The enhancement of turbulence is then capable of disrupting more efficiently the existing thermal stratification close to the ground, thereby increasing shimmering and consequently reducing the quality of astronomical observations.

3.3 Relative humidity analyses

On average throughout the year, relative humidity is about 15% at Paranal, but has an annual cycle in which maximum values are recorded in December and January, at the height of the southern hemisphere summer where moisture convergence raises the humidity levels beyond 30%. May is often slightly moister than October. Relative humidity values are frequently less than 5% on a monthly-average basis, however, which is characteristic of this extremely arid part of the word (Flugel and Chang, 1999).

During periods of lower than average seeing, relative humidity increases sharply in the northern part of the Chilean Andes, as a result of the advection of moist air. Figure 12 shows the concentration of relatively moist air at the 700 hPa level along the Peruvian Andes, and the curvature of this moist zone southwards into northern Chile. More detailed mesoscale analyses at the 300 hPa level suggest that air entrained from the NW may originate from the Bolivian region, cross over the Pacific offshore from Peru, and then flow in a south-easterly direction towards northern Chile (Erasmus, 1998).

Insert Figure 12 here

While on average, the relative humidity at Paranal is around 15% or less (see Figure 12b, for October 1994, for example), making it one of the driest regions of the planet, La Niña and associated atmospheric circulations serve to increase the values of relative humidity to around 40% in both the May 2000 and the October 1998 cases. While this may still be considered to be very dry compared to mid-latitude Europe, for example, this doubling of relative humidity nevertheless implies a substantial change in the presence of water vapor in the Andean atmosphere. Such an increase in moisture has the potential for thin cirrus cloud formations at higher elevations in the troposphere, which can lead to less favorable conditions for astronomical observations.

The relative humidity maps indicate that the northern part of the Chilean Andes experience the sharpest positive relative humidity anomalies anywhere over the South American continent. The source region of the moisture observed at the 700 hPa level, according to the synoptic analyses, may be located offshore from Peru and Ecuador, in a region confined within longitudes 80°-100°W and latitudes 5°-15°S. However, as discussed by Erasmus (1998), the moisture may actually originate in Bolivia and follow a circuitous route over Peru, out to the ocean, and then southwards back to Chile. Whatever its source, however, moisture convergence tends to increase relative humidity in much of the Andean chain; some of this high moisture spills over into the coastal ranges of northern Chile and thereby affects Paranal. The zones with above-average moisture stretches further south-eastwards into Argentina, well beyond the boundaries of the Andes, as discussed by Ruttland and Ulriksen (1979).

3.4 Cloud forcing net longwave flux analyses

The cloud forcing net longwave flux (CFNLF) allows an indirect assessment of the presence of clouds by integrating the changes in longwave terrestrial radiation between the ground surface and the upper atmosphere. Hence, an increase in the longwave flux in any given region signals the presence of some form of cloud liquid water or ice, which reduces the outgoing longwave radiation by increasing the opacity of the atmosphere to infrared wavelengths. It is also a parameter that is in some instances more useful than water vapor to describe perturbations to astronomical observations. Thus is because CLNWF is a measure of the possible presence of clouds when direct cloud observations are not possible, and which the analyses of relative humidity alone do not allow. While the CLNWF does not tell us anything about the type of cloud that may be present, it can be assumed that any small increase in its value may be associated with very thin high-altitude clouds, such as cirrus. These clouds are often undetected by the naked eye, but have the potential of disrupting precise astronomical observations by the VLT.

Insert Figure 13 here

Figure 13 shows the distribution of CFNLF over the central South America domain. While the core of elevated values of CFNLF is located to the NE of the ESO site, the values at Paranal range from 12-15 W/m^2, up from less than 9 W/m^2 in May 1994 (optimal seeing conditions for May) and 3 W/m^2 in October 1994 (optimal seeing conditions). The La Niña type of synoptic situation brings with it sufficient moisture to allow the formation of thin clouds above the ESO VLT site, with the consequent reduction of the astronomic observing conditions which this entails.

3.5 Consistency with other periods in which seeing conditions are lower than average

In order to confirm the systematic nature of the conclusions discussed above, a number of other situations with good or poor seeing conditions have been selected. The data are provided in tabular form in Table 1 for the months of May and October in which seeing conditions are either above or below average. The seeing parameter is on average 0.75 for the period of the observational record at Paranal, and one standard deviation (σ) is 0.113. Thus, any departure by at least 2σ or more can be considered to represent particularly good or particularly poor conditions for astronomical observations. On this basis, representative examples that have been chosen for good seeing conditions include May 1991 and, for less optimal conditions, October 1999. In the former case, the equatorial Pacific was in a normal phase preceding the 1992 El Niño outbreak, while the latter case is representative of the strong and persistent La Niña phase which followed the strongest 20th Century El Niño event of late 1997. This La Niña event was observable from the late Spring of 1998 and persisted until late 2000, which is an unprecedented duration for the cold ENSO phase.

Insert Table 1 here

Table 1 shows that there are indeed systematic differences between good and poor seeing periods. The height of the 700 hPa geopotential is generally lower under conditions of less than average seeing by up to 20 m (see for example October 1997 vs. October 1989), which represents a significant contraction of the atmosphere between the ground surface and the 700 hPa geopotential level. Wind velocities are on average higher during periods of less than average visibility but, more significantly, relative humidity and the associated cloud longwave radiative forcing are considerably higher, for the reasons evoked above.

Outside the time-frame of instrumental observations at Paranal, a survey has been made to assess whether similar synoptic situations leading to poor seeing conditions have been observed over the last 50 years. This has been achieved by analyzing the similarities in the distribution of geopotential height (700 hPa), wind velocity, relative humidity, and cloud forcing net longwave flux

since 1948, compared to the worst-case scenarios discussed here (October 1998, October 1999). The assessment has shown that the months of October of the following years exhibit conditions similar to the worst-case scenarios for astronomical observations: 1949, 1953, 1955, 1958, 1964, 1974, 1981, and 1990. Many, but not all, of these years are associated with La Niña events. It should also be emphasized that the NCEP re-analysis data in the vicinity of Antofagasta are of lower quality prior to the beginning of the upper-air soundings in the region in 1958.

Two events observed in September 1958 and October 1990, serve to highlight the fact that there have indeed been other periods in the past with similar climatic characteristics to the 1998-2000 situation. In this sense, these most recent years are not necessarily an exceptional feature in northern Chile, even though they significantly affect optimal seeing conditions.

Insert Figure 14 here

The salient features already seen in the detailed analyses of the May and October 1998 synoptic charts can be observed in a number of the earlier recorded cases, namely the north-westerly flow along the 700 hPa geopotential isolines (Figure 14 for October 1958), high relative humidity, stronger winds and enhanced cloud forcing net longwave radiation (Figure 15 for October 1990).

Insert Figure 15 here

It can thus be concluded from these selected examples, and from further analyses of other periods of good and poor astronomical observing conditions not illustrated here, that systematic climatological differences are seen to occur between periods where seeing conditions are either favorable or poor.

4. Conclusions

The principal conclusions of this study may thus be summarized as follows:

- The less than optimal conditions for astronomic observations that have prevailed since 1998 at the ESO VLT Paranal site are apparently not the result of a long-term warming trend in climate.
- The Paranal site is highly sensitive to ENSO forcing, despite its altitude and the fact that it lies well above the maritime boundary layer.

- The less than average seeing conditions are related to the onset of La Niña events. Atmospheric circulation changes and associated shifts in temperature and wind velocity seem to be the most likely cause for a reduction in the observing potential of the VLT.
- The presence of enhanced atmospheric moisture during La Niña events is potentially capable of increasing high-level cloudiness. Even thin cirrus-type clouds can perturb the quality of astronomical observations by the VLT.
- The lower than average seeing conditions experienced in 1998-2000 are not a unique event in the history of the Paranal site. By using the Antofagasta climatological record to extend, by analogy, the Paranal data back in time, it is seen that other periods in the past (e.g., 1958 and 1990) have exhibited similar behavior in 700 hPa airflow, wind velocity, temperature, and moisture content of the atmosphere. Had the VLT been operational at that time, astronomical observations would have probably been as disrupted as in 1998 and subsequent years.
- However, the particular severity of the 1998 La Niña event explains to a large extent the sequence of unfavorable seeing conditions
- Until predictions of ENSO events are improved, there is for the moment no certainty as to whether poor seeing conditions will recur and, if so, with which frequency.

5. Acknowledgements

The authors acknowledge the valuable contributions, through the datasets which they have made available for this study, Dr. John Eischeid (NOAA-CDC in Boulder, Colorado) and Cpt. Rodrigo Núñez G. (Servicio Hidrólogico y Oceanográfico de Chile). Thanks are also given to an anonymous reviewer for providing very constructive comments that have helped improve the original manuscript.

The NCEP Reanalysis data is provided by the NOAA-CIRES Climate Diagnostics Center, Boulder, Colorado, USA, from their Internet site at http://www.cdc.noaa.gov/ for the 2-dimensional surface plots of geopotential height, relative humidity, cloud forcing net longwave flux, wind speed and sea surface temperature. The public availability of data (Southern Oscillation Index) from the Climate and Global Dynamics Division of the University Corporation for Atmospheric Research (UCAR/CGD on URL: http://www.cgd.ucar.edu/cas/catalog/climind/soi.html) and the software package GrADS from the Center for Ocean-Land-Atmosphere Studies (COLA on URL: http://grads.iges.org/grads/) are gratefully acknowledged.

This study has been undertaken under contract with the European Southern Observatory (ESO) contract number: 61243 / ODG / 00 / 8543 / GWI / LET .

6. References

Aceituno, P., H. Fuenzalida, and B. Rosenbluth, 1993: Climate along the extratropical west coast of South America. In: Part II: Climate Controls. Earth System Responses to Global Change: Contrasts Between North and South America [Mooney, H., E. Fuentes, and B. Kronberg (eds).]. Kluwer Academic Publishers, Dortrecht, The Netherlands, pp. 61-72

Barros, V., M.E. Castañeda, and M. Doyle, 1999: Recent precipitation trends in South America to the east of the Andes: an indication of climatic variability. In: Southern Hemisphere Paleo and Neoclimates: Concepts and Problems [Volheimer, W. and P. Smolka (eds.)]. Springer-Verlag, Berlin and Heidelberg, Germany

Cantañeda, M.E. and V. Barros, 1993: Las tendencias de precipitación en el Cono Sur de América al este de los Andes. Meteorológica, 19

Compagnucci, R.H., 1991: Influencia del ENSO en el desarrollo socio económico de Cuyo. In: Anales CONGREMET VI, 23-27 March 1991, Buenos Aires, Argentina. Centro Argentino de Meteorólogos, Argentina, pp. 95-96

Compagnucci, R.H., 2000: Impact of ENSO events on the hydrological system of the Cordillera de los Andes during the last 450 years. In: Southern Hemisphere Paleo and Neoclimates: Concepts, Methods and Problems [Volheimer, W. and P. Smolka (eds.)]. Springer-Verlag, Berlin and Heidelberg, Germany

Compagnucci, R.H. and W.M. Vargas, 1998: Interannual variability of the Cuyo River's streamflow in the Argentinian Andean mountains and ENSO events. International Journal of Climatology, 18, 1593-1609

Diaz, H. F. and Graham, N. E., 1996: Recent changes in tropical freezing heights and the role of sea-surface temperature. Nature, 383, 152-155..

Eltahir, E.A.B., and G. Wang,1999: El Niño and climate variability. Geophysical Research Letters, 26, 4, 489.

Erasmus, D. A., 1998: The effects of El Niño - Southern Oscillation on the seasonal, inter-annual and spatial variability of water vapour and cirrus cloud cover over Northern Chile. A Satellite-Derived Climatology of Water Vapour and Cirrus Cloud Cover in the Area of Chajnantor, Northern Chile . This document can be found at the following URL: http://www.eso.org/genfac/pubs/astclim/espas/radioseeing/erasmus/proposal1.htm

ESO, 2001: http://www.eso.org/gen-fac/pubs/astclim/paranal/index.html

Flugel, M., and P. Chang, 1999: Stochastically induced climate shift of El Niño-Southern Oscillation phenomenon. Geophysical Research Letters, 26, 16, 2473-2476

Garreaud, R. and J. Ruttland, 1996: Análisis meteorológico de los aluviones de Antofagasta y Santiago de Chile en el periódo 1991-1993. Atmósfera, 9, 251-271

Garreaud, R. And P. Aceituno, 2001: Interannual rainfall variability over the South American Altiplano. J. Clim, 14, 2779-2789

Garreaud, R., and D. Battisti, 1999: Interannual (ENSO) and interdecadal (ENSO-like) variability in the Southern Hemisphere tropospheric circulation. Journal of Climate, 12, 7, 2113-2123.

Giorgi, F., Hurrell, J., Marinucci, M., and Beniston, M., 1997: Height dependency of the North Atlantic Oscillation Index. Observational and model studies. J. Clim., 10, 288 – 296

Hoffman, J.A.J., T.A. Gomez, and S.E. Nuñez, 1987: Los campos medios anuales de algunos fenómenos meteorológicos. In: II Congreso de Meteorología. CAM, AMS, SBM, OMMAC, and SOCOLMET, Buenos Aires, Argentina

Hunt, A.G., 1999: Understanding a possible correlation between El Niño occurrence frequency and global warming. Bulletin of the American Meteorological Society, 80, 2 , 297-300.

Jones, P.D., New, M., Parker, D.E., Martin, S. and Rigor, I.G., 1999 : Surface air temperature and its changes over the past 150 years. Reviews of Geophysics, 37, 173-199

Jungo, P., and Beniston, M., 2001: Changes in the anomalies of extreme temperature anomalies in the 20th Century at Swiss climatological stations located at different latitudes and altitudes. Theor. and Appl. Clim., 69, 1-12

Karl, T. R., Jones, P. D., Knight, R. W., Kukla, G., Plummer, N., Razuvayev, V., Gallo, K. P., Lindseay, J., Charlson, R. J., and Peterson, T. C., 1993: Asymmetric trends of daily maximum and minimum temperature. Bull. American Meteorol. Soc., 74, 1007 - 1023

McPhaden, M.J., 1999: Genesis and evolution of the 1997-98 El Niño. Science, 283, 950-954.
Minetti, J.L. and E.M. Sierra, 1989: The influence of general circulation patterns on humid and dry years in the Cuyo Andean region of Argentina. International Journal of Climatology, 9, 55-69
Moore, A., and R. Kleeman, 1999: The non-normal nature of El Niño and intraseasonal variability. Journal of Climate, 12, 10, 2965-2982.
Rosenblüth, B., Fuenzalida, H. A., and Aceituno, P., 1997: Recent Temperature variations in Southern South America. Int. J. Climatology, 17, 67-86
Ruttland, J. and H. Fuenzalida, 1991: Synoptic aspects of the central Chile rainfall variability associated with the Southern Oscillation. International Journal of Climatology, 11, 63-76
Ruttland, J. And P. Ulriksen, 1979: Boundary-layer dynamics of the extremely arid northern part of Chile: The Antofagasta field experiment. Boundary-Layer Meterorol., 17, 41-55
Salles, M.A. and R.H. Compagnucci, 1997: Características de la circulación de superficie durante el período diciembre de 1971-febrero de 1974 y sus relaciones con las anomalías ENSO en el sur de Sudamérica. Meteorológica, 22, 35-48
Van Loon, H., Taljaard, J ., Sasamori, T., London, J., Hoyt, D. V., Lavitzke, K., and Newton, C. W., 1972: Meteorology of the Southern Hemisphere. Monograph Volume 13, 35, American Meteorol. Soc., Boston, Mass.
Vuille, M., and Bradley, R. S., 2000: Mean annual temperature trends and their vertical structure in the tropical Andes, Geophys. Res. Lett., 27, 3885-3888
Vuille, M., Bradley, R. S., and Keimig, F., 2000: Climate variability in the Andes of Ecuador and its relation to tropical Pacific and Atlantic sea surface temperature anomalies. J. Clim., 13, 2520-2535
Waylen, P. and C. Caviedes, 1990: Annual and seasonal fluctuations of precipitation and streamflow in the Aconcagua river basin, Chile. Journal of Hydrology, 120, 79-102
Wolter K., and M.S. Timlin, 1998: Measuring the strength of ENSO events - how does 1997/98 rank? Weather, 53, 220-242

Figure Captions; Table Caption

Figure 1: Map of Chile showing the location of the Paranal VLT site.
Figure 2: Time series of seeing conditions at the Paranal VLT site.
Figure 3: Diagram highlighting periods with above or below normal seeing condtions, from 1987-2001.
Figure 4: Correlation of Paranal mean temperature series with Antofagasta mean temperature series, 1985-2001.
Figure 5: Upper-air sounding at Antofagasta in May 1994 (good seeing) and May 2000 (poor seeing), illustrating the strong inverstion layer and the changes in temperature at the altitude of Paranal (dashed horizontal line) that intervene during good and poor seeing conditions.
Figure 6: 50-year time series for mean temperature at Antofagasta (dashed line), used to extend the Paranal record back in time (bold line).
Figure 7: a-Upper) Geopotential height of the 700 hPa level for May 2000; b-Lower) Geopotential height of the 700 hPa level for October 1998. Both figures for the eastern Pacific-South America-South Atlantic domain.
Figure 8: a-Upper) Geopotential height of the 700 hPa level for May 2000; b-Lower) Geopotential height of the 700 hPa level for October 1998. Both figures for the central segment of South America. Target locates the Paranal VLT site; arrow indicates the general flow direction at Paranal.
Figure 9: a-Upper) Geopotential height of the 700 hPa level for May 1994; b-Lower) Geopotential height of the 700 hPa level for October 1994. Both figures for the eastern Pacific-South America-South Atlantic domain.
Figure 10: a-Upper) Geopotential height of the 700 hPa level for May 1994; b-Lower) Geopotential height of the 700 hPa level for October 1994. Both figures for the central segment of South America. Target locates the Paranal VLT site; arrow indicates the general flow direction at Paranal.
Figure 11: Upper-air sounding at Antofagasta for wind velocity profiles in May and October 1994 (good seeing), and October 1998 and May 2000 (poor seeing), and the changes in the profiles at the altitude of Paranal (dashed horizontal line) that intervene during good and poor seeing conditions.
Figure 12: a-Upper) Relative humidity at the 700 hPa level for October 1998; b-Lower) Relative humidity at the 700 hPa level for October 1994. Both figures for the central segment of South America. Target locates the Paranal VLT site. Values of relative humidity at Paranal for October 1998: 39%; for October 1994: 17%.
Figure 13: a-Upper) Cloud forcing net longwave radiation (CFNLR) for October 1998; b-Lower) Cloud forcing net longwave radiation (CFNLR) for October 1994. Both figures for the central segment of South America. Target locates the Paranal VLT site. Values of CFNLR at Paranal for October 1998: 14 W/m^2; for October 1994: 3.5 W/m^2.
Figure 14: Geopotential height of the 700 hPa level for May 1958. Target locates the Paranal VLT site; arrow indicates the general flow direction at Paranal.
Figure 15: Cloud forcing net longwave radiation (CFNLR) for October 1990. Target locates the Paranal VLT site. Values of CFNLR at Paranal: 11 W/m^2.

Table 1: Values of geopotential, wind speed, relative humidity and cloud forcing net longwave flux (CNLWF) for periods in May and October with below average (normal text) and above average (bold script) seeing conditions. Gray shading highlights the best-case and worst-case scenarios discussed in the text.

Beniston et al., 2002: Table 1

	Months of May									
	1989	**1991**	**1994**					1998	1999	2000
Seeing	**.638**	**.596**	**.575**					.728	.866	.896
Geopotential	**3145**	**3148**	**3145**					3140	3138	3130
Wind speed	**5.0**	**4.6**	**4.8**					4.1	4.3	5.2
Rel humidity			**22**							37
Cloud LW	**7**	**8**	**9**					8	8	11
	Months of October									
	1989	**1990**	**1994**	**1995**	1988	1996	1997	1998	1999	2000
Seeing	**.694**	**.625**	**.544**	**.675**	.761	.712	.703	1.053	0.984	0.719
Geopotential	**3140**	**3139**	**3132**	**3130**	3129	3129	3120	3132	3128	3126
Wind speed	**3.5**	**5.0**	**4.4**	**3.9**	4.2	4.2	6.5	5.5	5.4	3.5
Rel humidity			**17**					42		
Cloud LW	**6**	**10**	**3**	**5**	3	4	8	14	12	8

M. Beniston et al., 2002: Figure 1

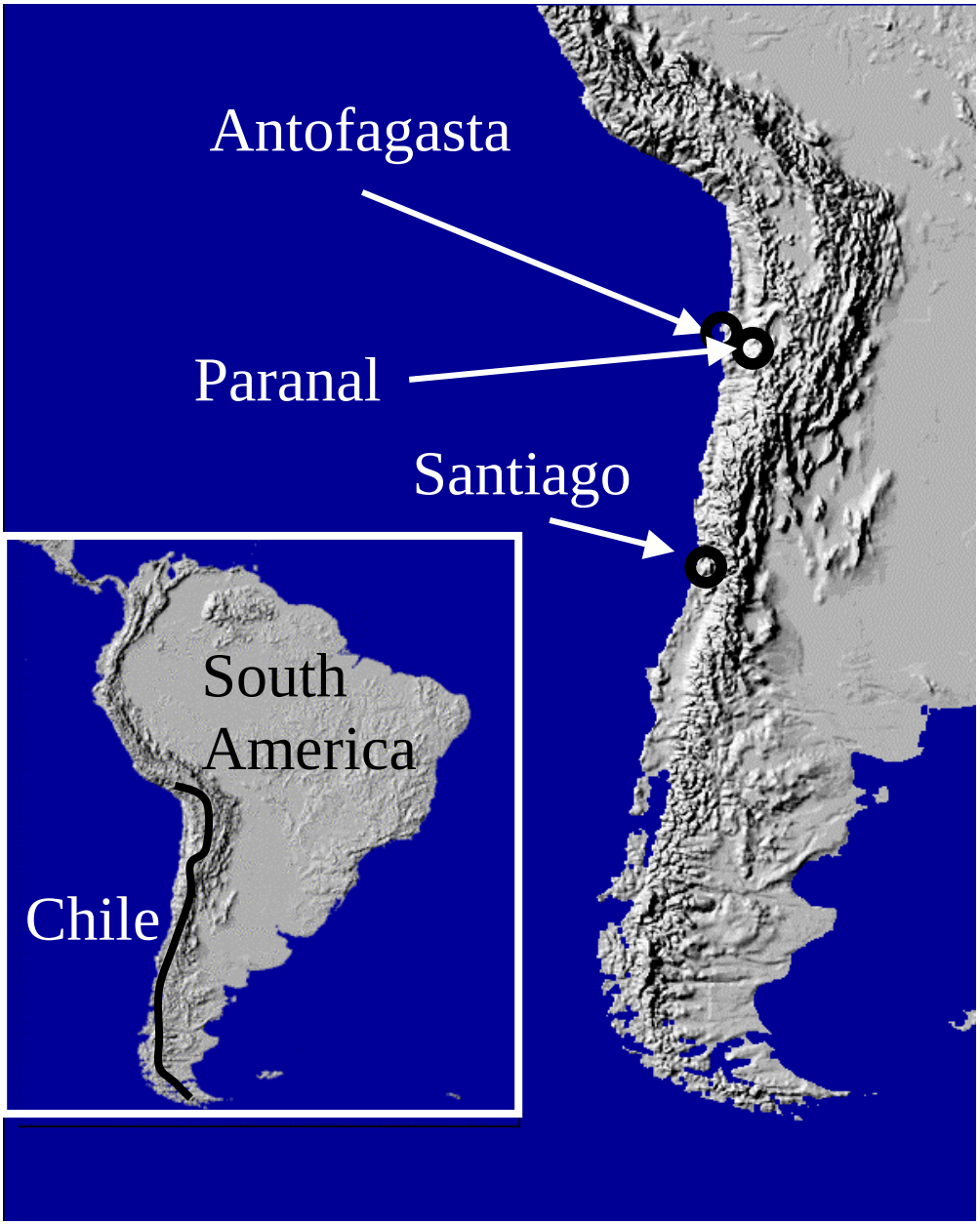

M. Beniston et al., 2002: Figure 2

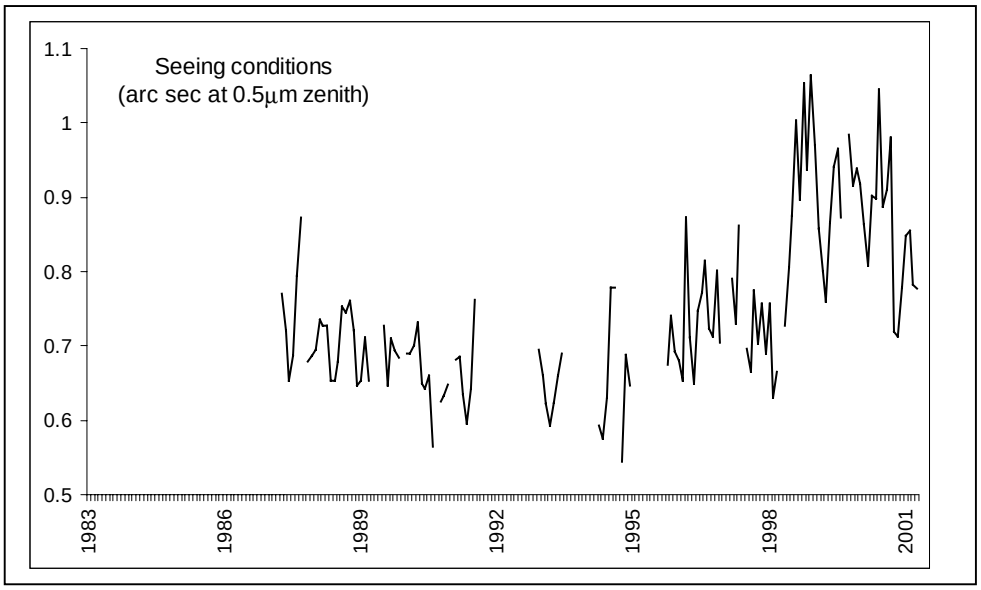

M. Beniston et al., 2002: Figure 3

	Jan	Feb	Mar	Apr	May	Jun	July	Aug	Sep	Oct	Nov	Dec
1987												
1988												
1989												
1990												
1991												
1992												
1993												
1994												
1995												
1996												
1997												
1998												
1999												
2000												
2001												

Poor conditions	
Fair conditions	
No data	

M. Beniston et al., 2002: Figure 4

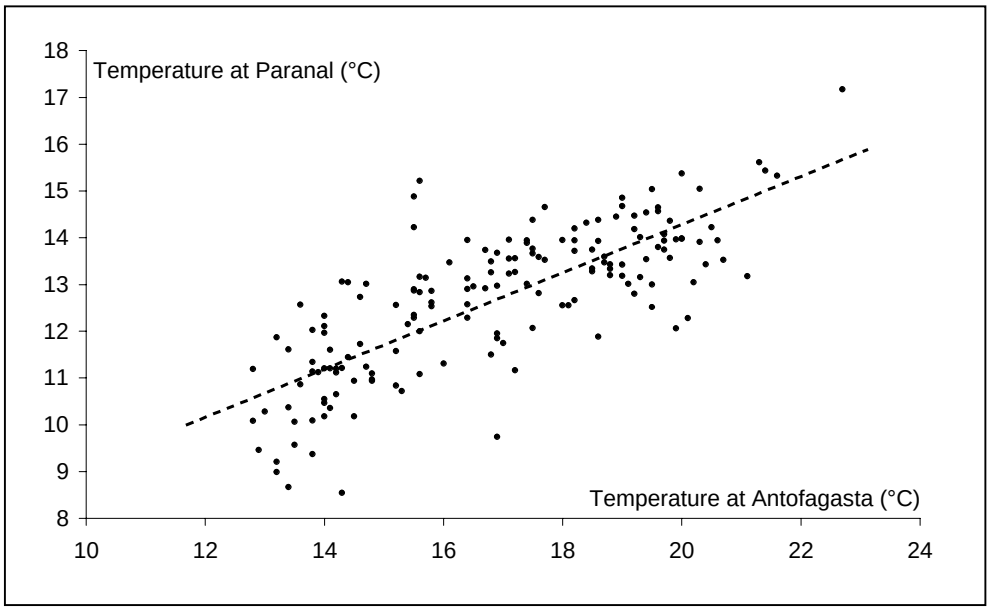

M. Beniston et al., 2002: Figure 5

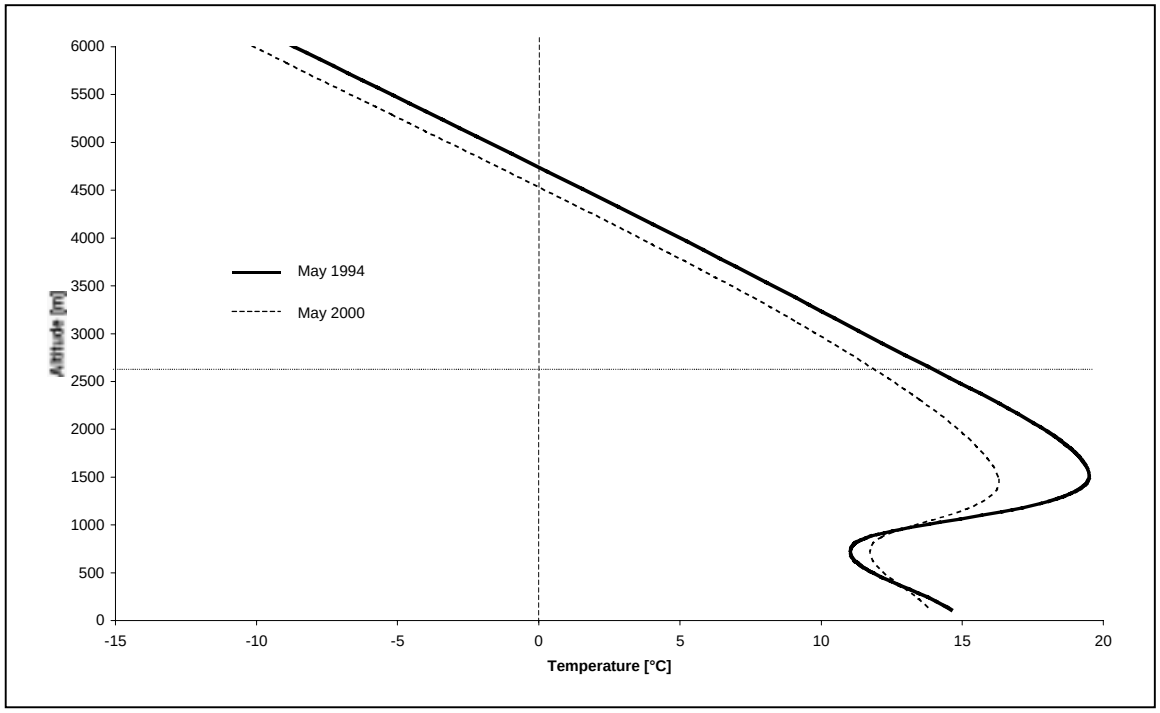

M. Beniston et al., 2002: Figure 6

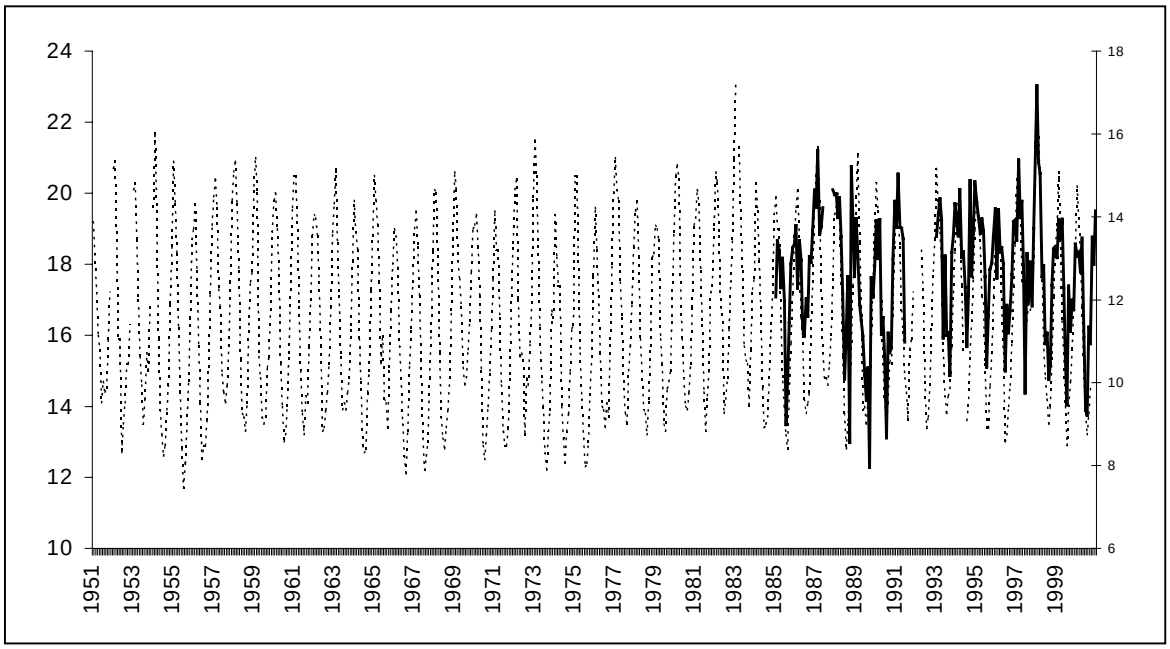

M. Beniston et al., 2002: Figure 7

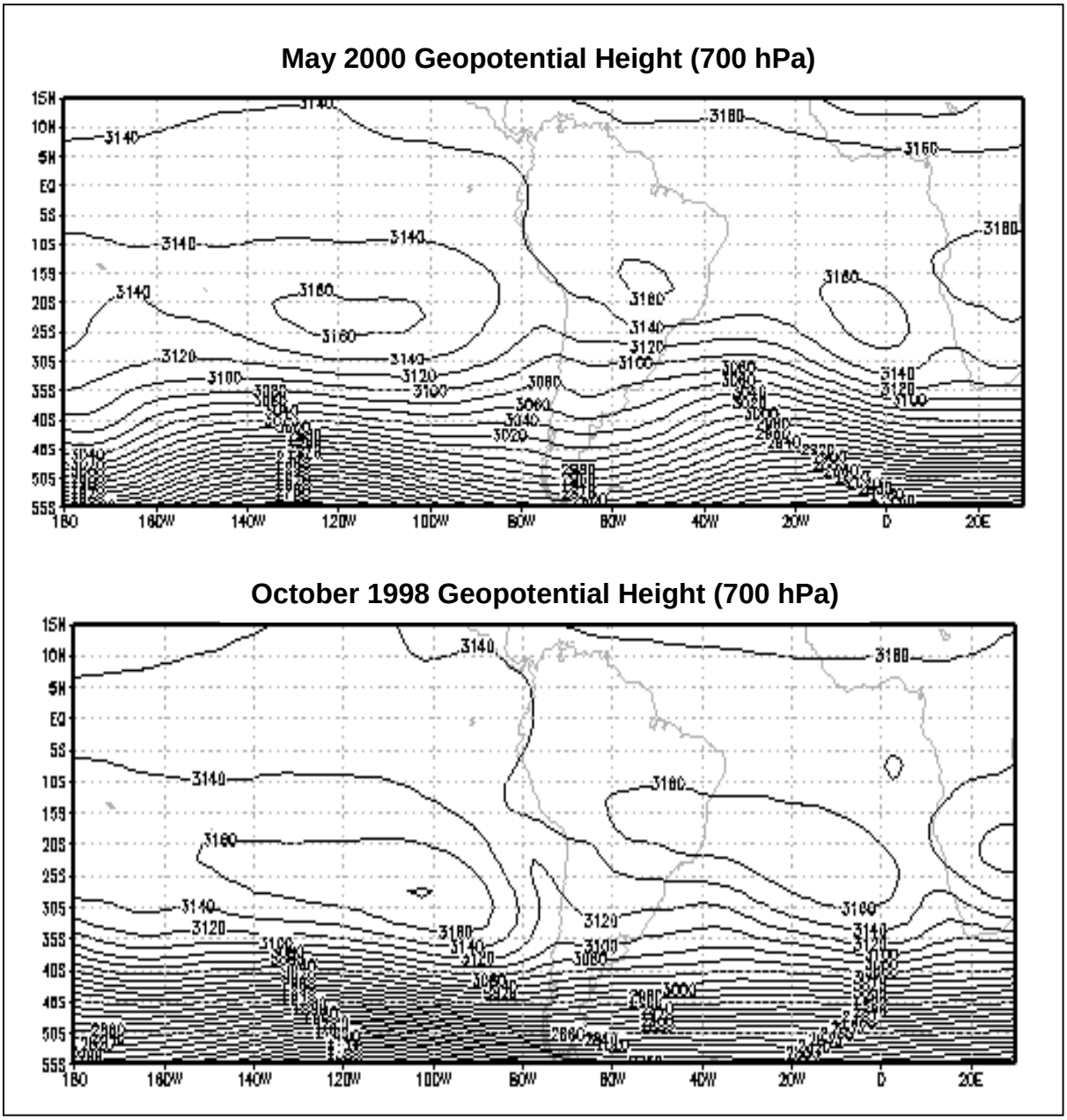

M. Beniston et al., 2002: Figure 8

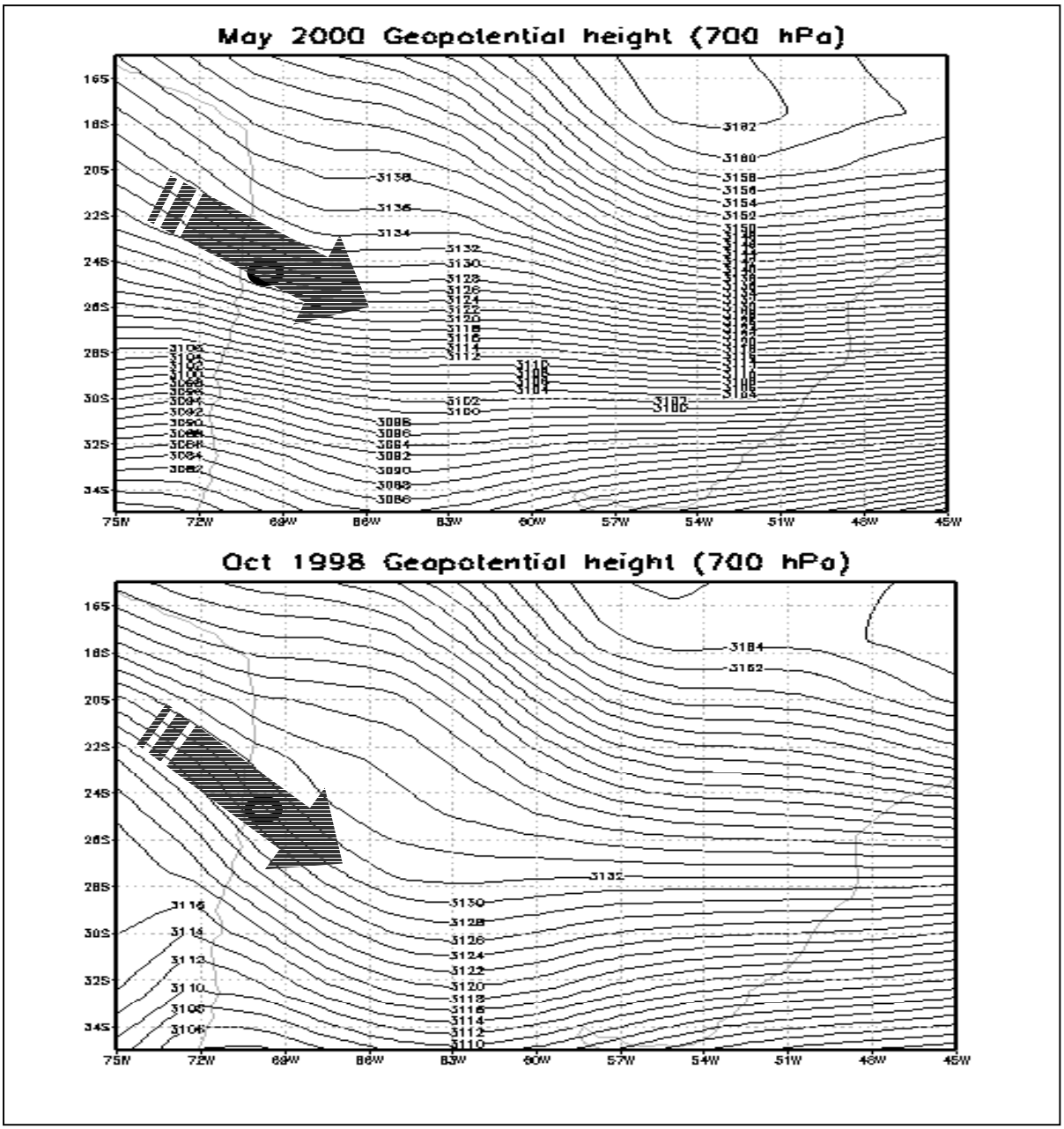

M. Beniston et al., 2002: Figure 9

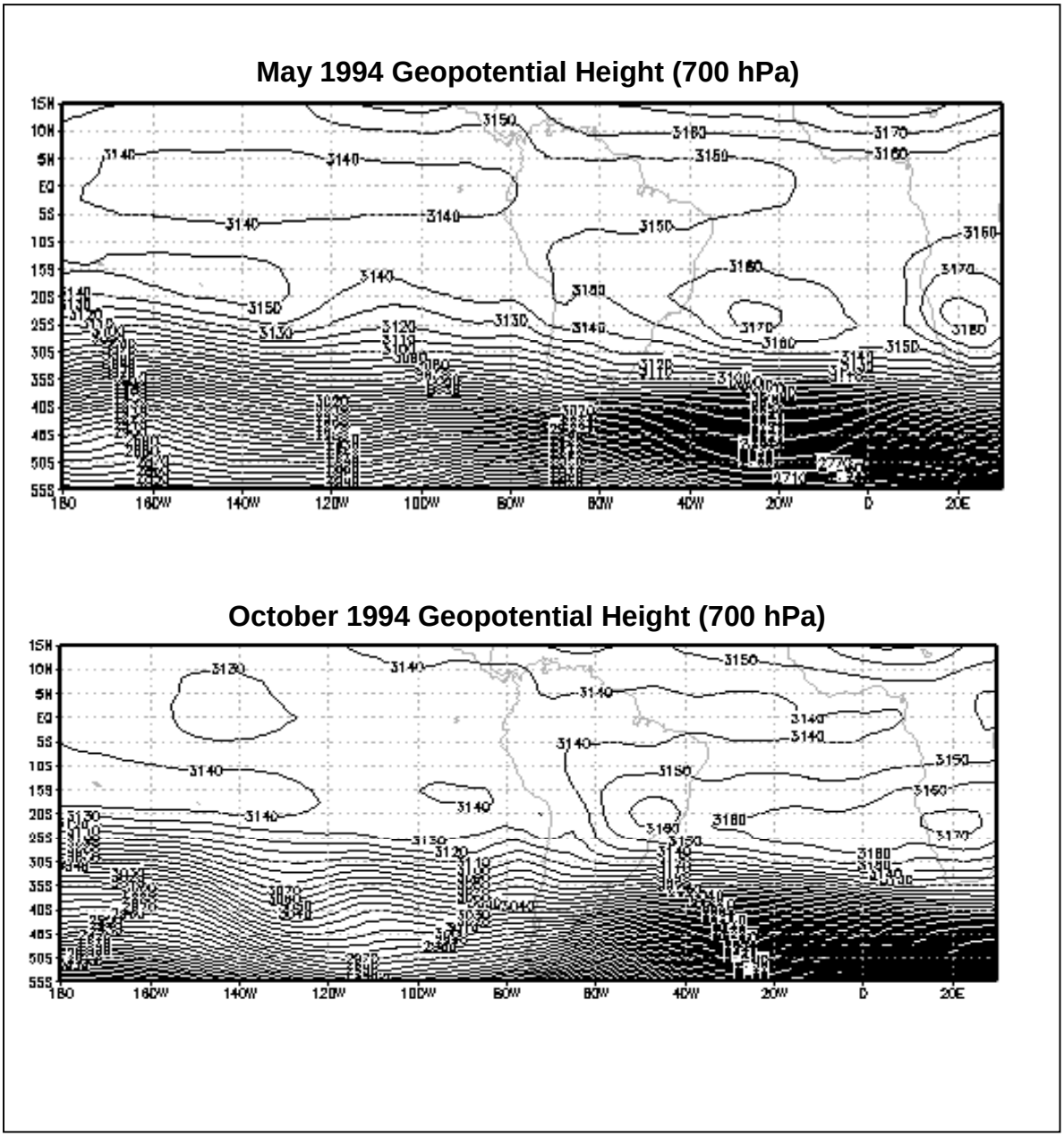

M. Beniston et al., 2002: Figure 10

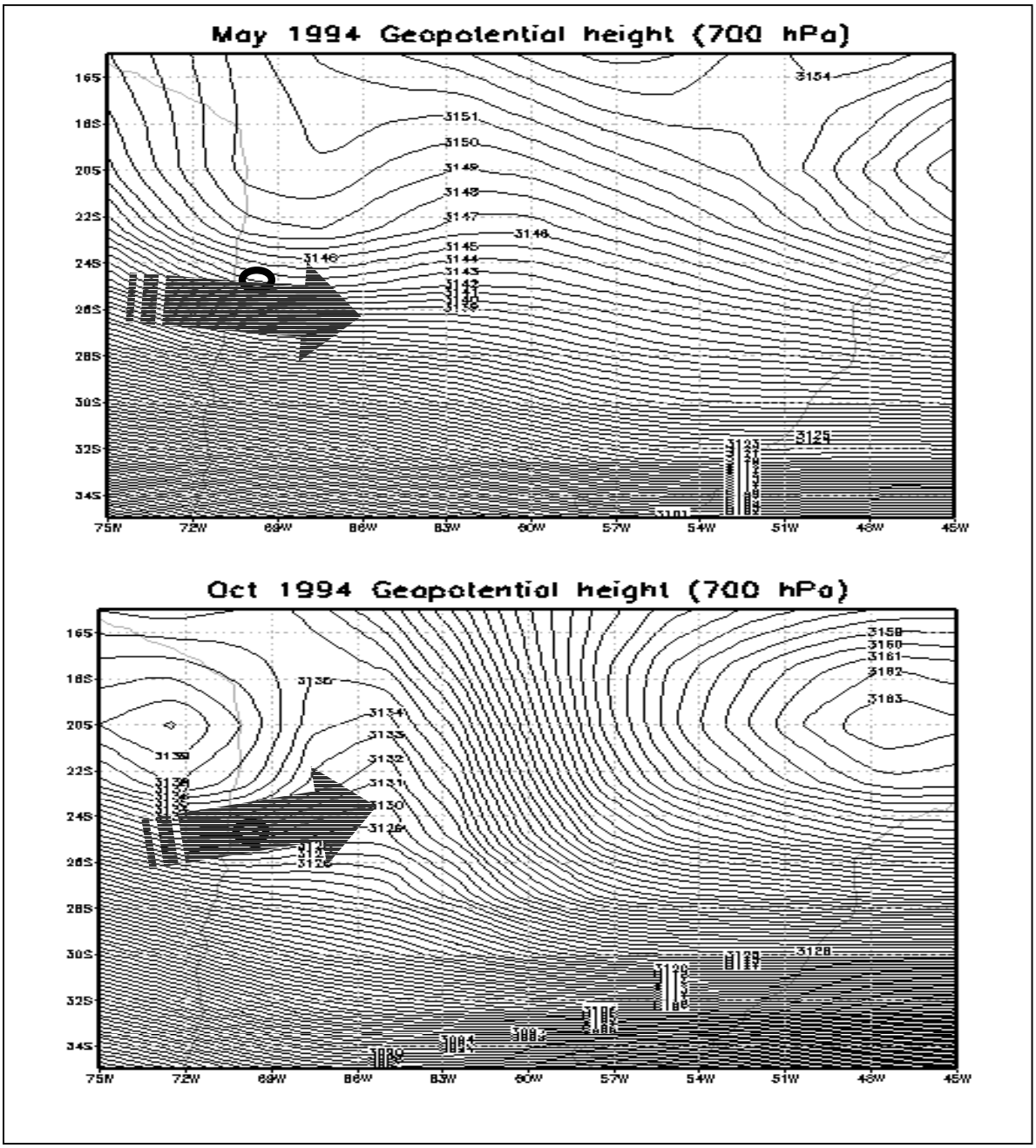

M. Beniston et al., 2002**:** Figure 11

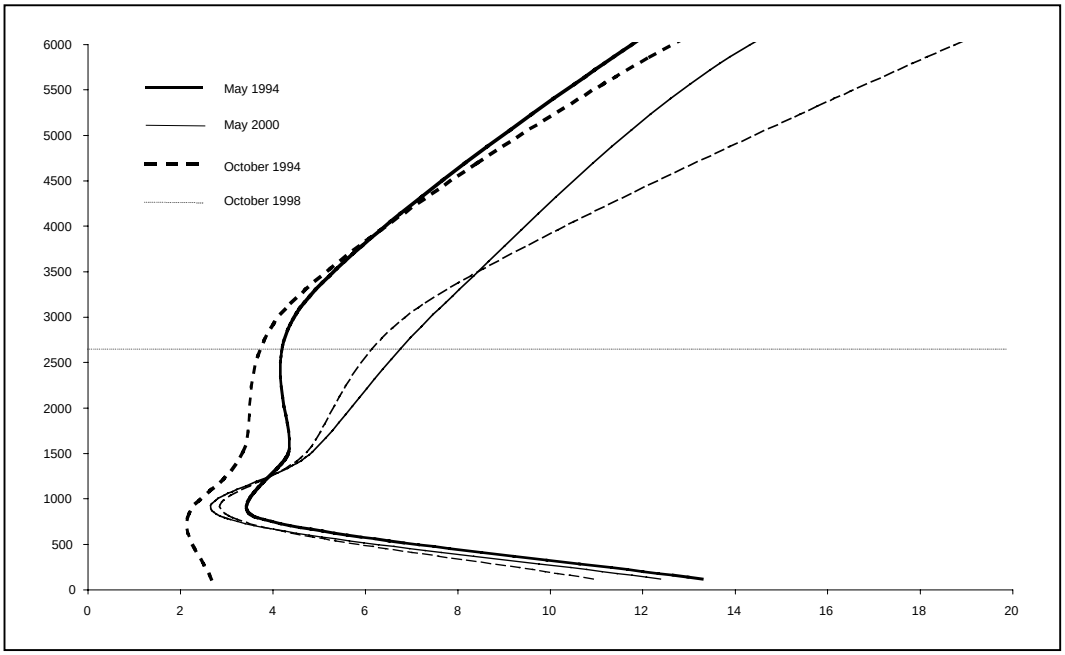

M. Beniston et al., 2002: Figure 12

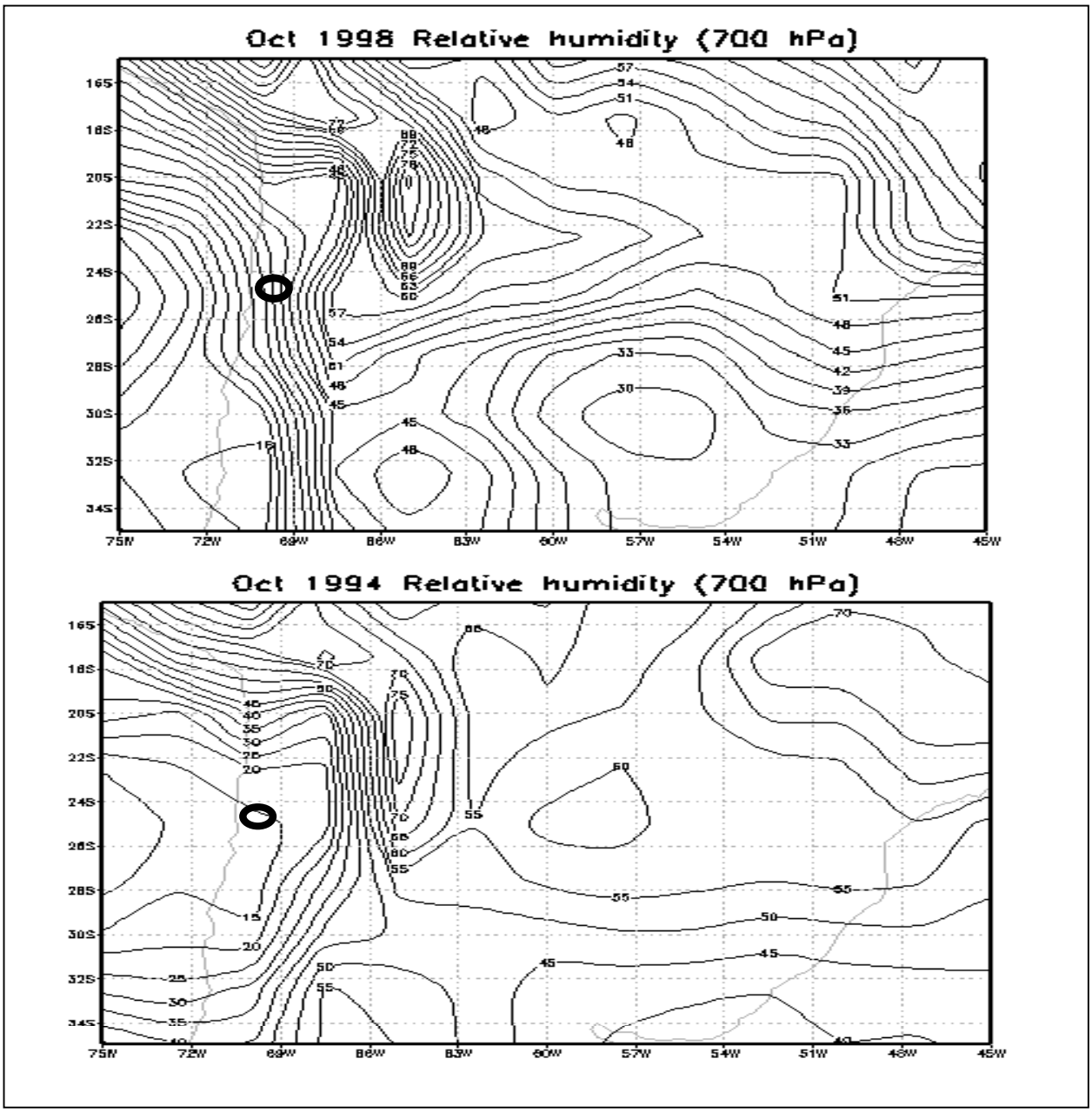

M. Beniston et al., 2002: Figure 13

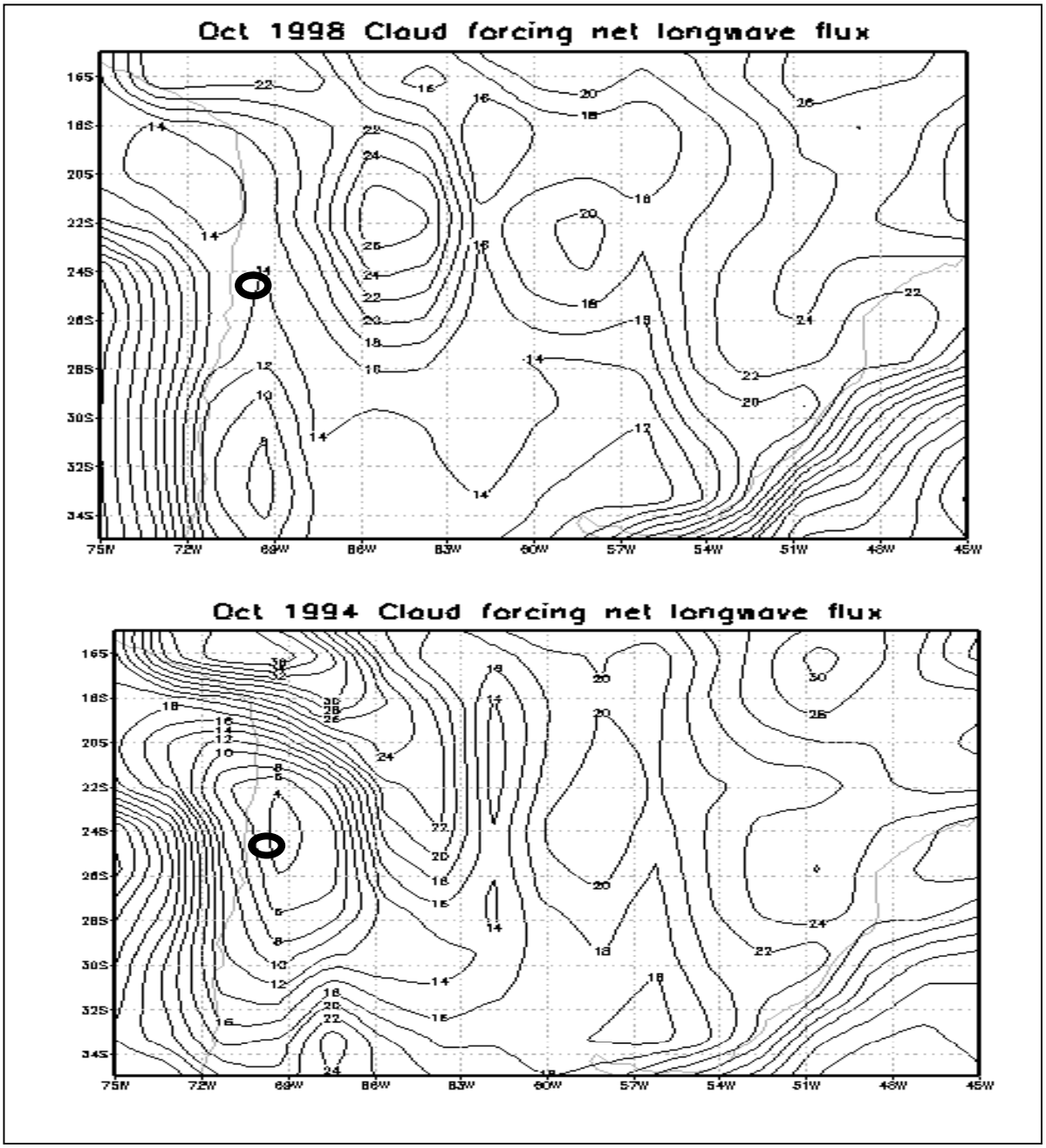

M. Beniston et al., 2002: Figure 14

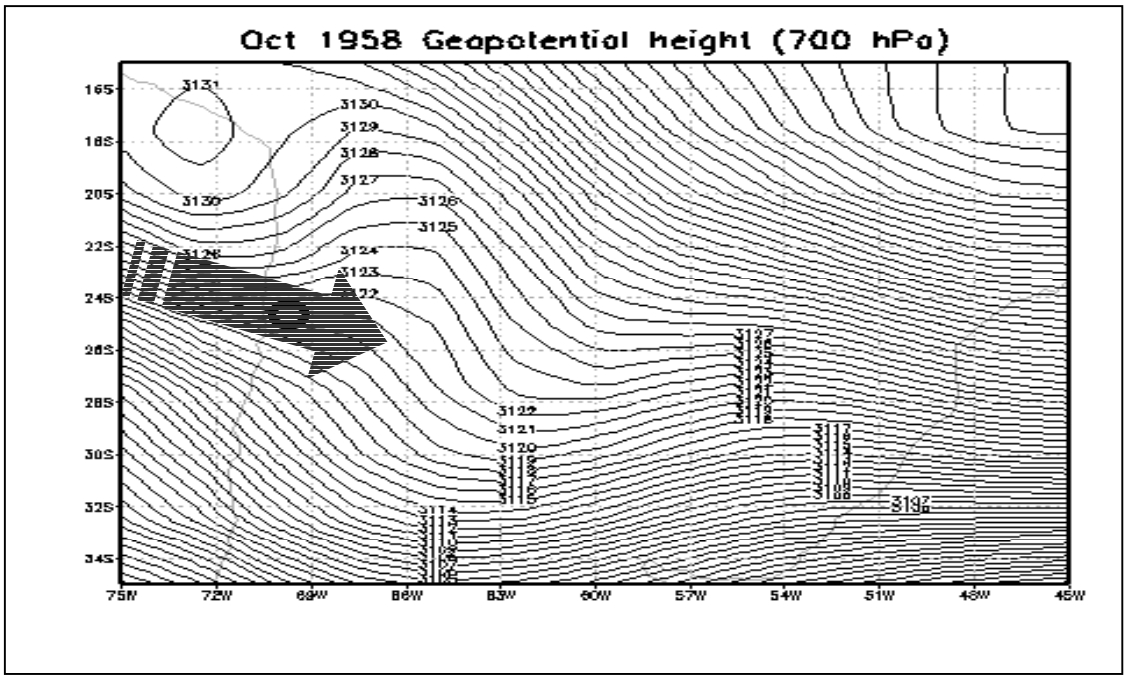

M. Beniston et al., 2002: Figure 15